Applied and Computational Mechanics 5 (2011) 197–204

A design influence on the mechanical compliance and fracture resistance of railway wheel

P. Navrátil[a,*], P. Janíček[a], L. Brabenec[a], M. Matug[a], P. Marcián[a]

[a] *Institute of Solid Mechanics, Mechatronics and Biomechanics, Faculty of Mechanical Engineering, Brno university of Technology, Technická 2896/2, 616 69 Brno, Czech Republic*

Received 13 November 2010; received in revised form 17 October 2011

Abstract

A fracture mechanics approach is used to determinate crack behaviour in a railway wheel which is working under different operating conditions with consideration of different types of railway wheel discs. Reliability of the railway wheel is related to a material failure. This paper is focused on failure of the material which is connected with violation consistency of the wheel material. The fracture mechanic approach is applied with consideration of influence of mechanical compliance. The topology optimization is used to define the shape of one disc type. Obtained results show fracture behaviour and the mechanical compliance of used railway wheel discs. From these results, comparison of separated railway wheel discs is obtained.

Keywords: fracture mechanics, mechanical compliance, railway wheel

1. Introduction

Since the beginning of the rail transport, the surface initiated by rolling contact fatigue (RCF) presented in railway wheels has been observed. These cracks can branch into thin layers of 0.5–5 mm under railway wheel (further referred to as RW) surface; this behaviour was studied by Ekberg [1]. Presented research attempts to predict the crack under non-proportional loading [4–7]. The crack can head to a wheel centre and then it can cause wheel destruction, or it can head to a wheel edge and cause spalling. In this paper, the crack that heads to the RW's centre is considered. The intensity of the crack propagation due to the RW cross-section profile for straight crack as a response to rolling contact loading is studied [2]. The FE simulations are used for predictions of the crack propagation [3].

2. Materials and methods

In order to determine crack behaviour, the finite element method for the computational simulation is used. The FEM is the most common numeric method used for solving problems in solid mechanics. For all analyses, the Ansys software (Ansys Inc., Canonsburg, PA, USA) is used. The model is defined from different points of view: the model of geometry, the model of materials, the model of boundary conditions and loads for two main cases, i.e. Mechanical compliance simulation and the Crack analysis simulation.

*Corresponding author. Tel.: +420 605 109 823, e-mail: ynavra26@stud.fme.vutbr.cz.

2.1. Model of geometry

For all simulations, a geometry model of the wagon's RW, i.e. the common wheel profile according to the European standards, is used. The straight profile, the arc profile and the profile obtained from topology optimization are used as additional models of the geometry.

2.1.1. Mechanical compliance simulation

The mechanical compliance is studied in this part. Solid RWs with a different geometry of the RW disc are assumed. The rail is assumed to be UIC 60 standard with $1 : 40$ cant to the RW. For the FEM mesh, common contact elements and 3D quadratic 20 node solid elements known as SOLID 186 are used. Topology optimization is a special case of the simulation. From the 2D simulation, a skew shape of the RW disc is obtained.

2.1.2. Crack analysis simulation

In this part, the fracture behaviour of the straight primary crack in the full 3D is studied. The cross-sections of wheel profiles are used as in previous simulation. Wheel with violated consistency caused by the straight crack perpendicular to wheel edge is taken into consideration. The crack is located in the disc part of the RW. The crack is considered to be primary with the straight crack path. The crack crosses whole cross-section of the RW. This is a major simplification of crack which is created. The length of the crack is considered to be from 330 mm (the shortest) to 210 mm (the longest) as can be seen in Fig. 1.

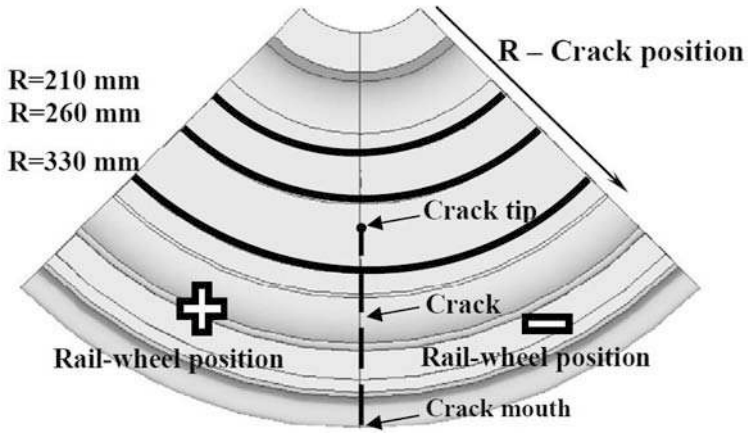

Fig. 1. Main spots on the RW disc

2.2. Model of material

For all load cases, the same type of the material is considered. The material of the wheel is assumed to be homogeneous, isotropic and linearly elastic. The rail is assumed to be rigid. Used material characteristics are following: Young's modulus $E = 210\,000$ MPa, Poisson's ratio $\nu = 0.3$ and fracture toughness $K_{\mathrm{IC}} = 80\ \mathrm{MPa} \cdot \mathrm{m}^{1/2}$. It is necessary to take into consideration the fracture toughness dynamic value which is approximately $K_{\mathrm{Id}} = 0.6 \cdot K_{\mathrm{IC}}$. The friction coefficient between two steel materials is considered as $f = 0.2$.

2.3. Model of boundary conditions and loads

Several conditions are applied in FEM simulations, because three types of simulations are done. The first one — the topology optimization, the second one — the mechanical compliance optimization, and the last one — the fracture analysis of the RW.

2.3.1. Topology optimization

The topology optimization is used as an auxiliary simulation for the mechanical compliance analysis. For this simulation, the optimization function is defined as a mass reduction of the RW disc in order to achieve maximum stiffness. Volume reduction up to 75 % is defined as a second optimization function. For the case of topology optimization, an axisymmetric 2D approach is considered. For this simulation, the 2D topology optimization is used, because a very fine mesh is necessary in order to achieve the most exact shape. The loading set is formed from two loading forces in mutual ratio. The chosen ratio of radial and axial forces is changed from low influence of axial force to double value of the axial force opposite to the radial force in order to find the most suitable profile.

2.3.2. Mechanical compliance simulation

For this type of optimization, the full 3D model of the RW is used. In this simulation the displacements in the wheel hub are set to zero. The two loading types are taken into consideration. The first load is assumed to have a radial direction, and the second, to have an axial direction. This load is applied into the contact spot of the RW and rail. The rail is considered to be rigid rail with the pilot node. The force load value is 10^5 N in both directions.

2.3.3. Crack analysis simulation

As previously, this simulation is realized by a full 3D geometry of the RW. Contrary to the previous simulation mentioned in 2.3.2, radial displacement equal to used interference fit in the RW hub is assumed in this analysis. Two maximum values of interference fit, the H7/r6 and H7/u6, are used. Three load cases are considered as force loading: the rectilinear ride, the acceleration and the braking case of the ride. The force in normal direction is considered as 10^5 N as in previous case, but contrary to the previous case, the tangential force is assumed as $0.2 \cdot 10^5$ N. The inertia forces caused by the wheel rotation are considered. The speed of the train is assumed to be 100 km/h, i.e. approximately 60.39 rad/s.

3. Results and discussion

3.1. Topology optimization

The set of several possible wheel discs is obtained as a result of topology optimization. The main difference among obtained profiles is in different ratios of axial/radial loading. Several examples are shown in Fig. 2.

The profile marked as b) in Fig. 2 — a skew shape profile is chosen for the simulations. The other shapes are chosen as non-suitable for the analysis. Shapes marked as c) and d) in Fig. 2 are obtained for very high influence of axial forces. On the contrary, the shape in Fig. 2a) is suitable for minimal influence of axial forces.

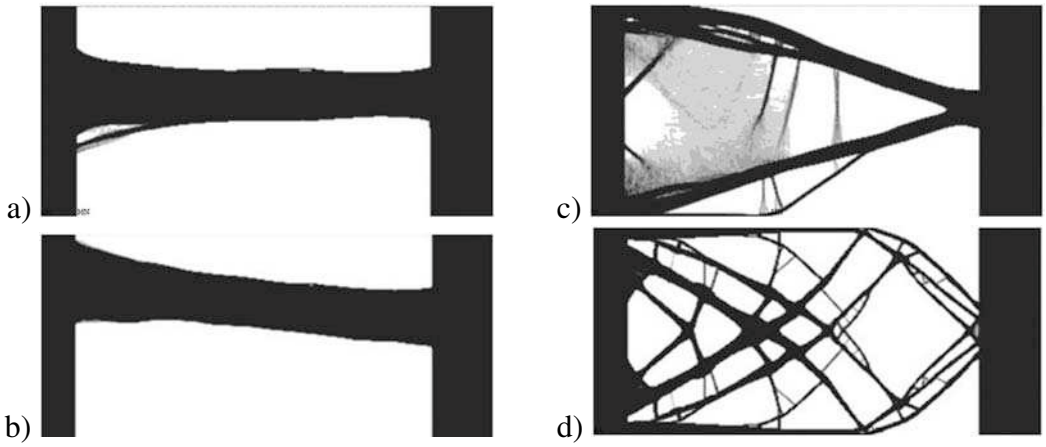

Fig. 2. Examples of results obtained from topology optimization

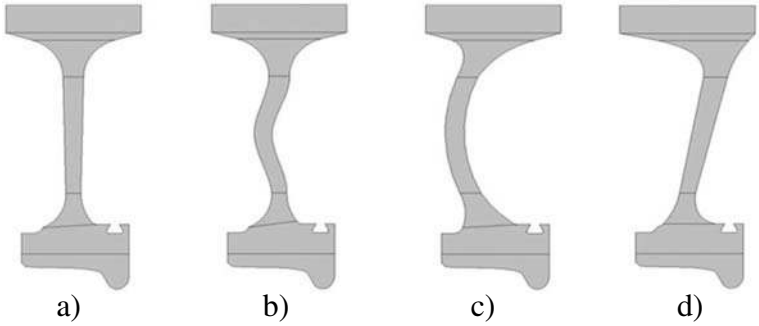

Fig. 3. Cross-sections of RW profiles considered in this paper: a) straight profile, b) classic profile, c) arc profile, d) skew profile

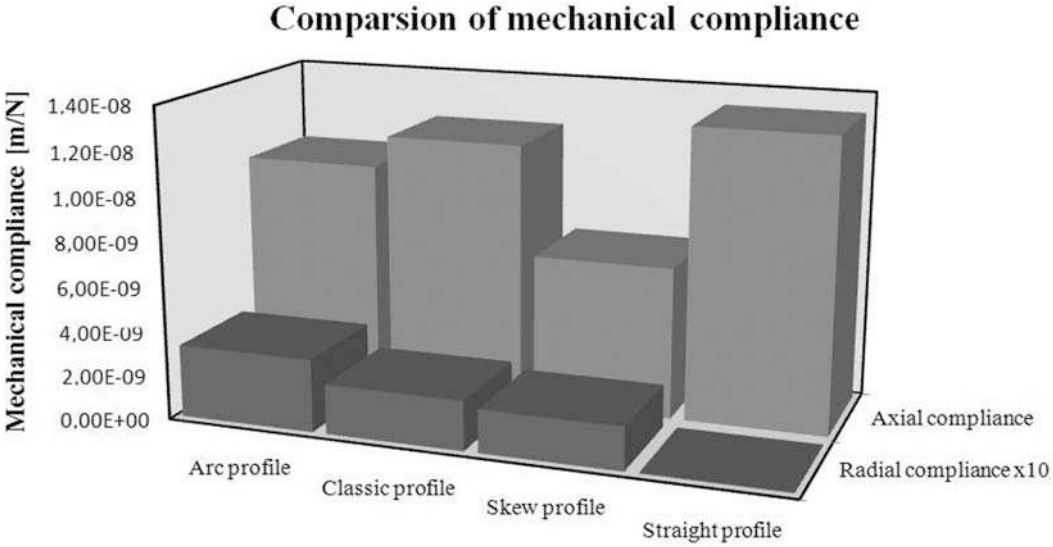

Fig. 4. Comparison of the mechanical compliance in different directions

3.2. Mechanical compliance simulation

The mechanical compliance of each profile is computed and the results are compared mutually for all considered cross sections (Fig. 3). Values of mechanical compliance are obtained from displacement results (Fig. 4).

In Fig. 4, it can be noticed that the radial mechanical compliance is much lower than compliance in the axial direction. This difference is caused by geometry of railway wheel.

3.3. Crack analysis simulation

In this simulation, the approach of linear elastic fracture mechanics is utilized, e.g. the crack behaviour is determined by using stress intensity factors (further referred to as SIF) K_{I}, K_{II} and K_{III}. The implement function called KCALC to evaluate SIFs in ANSYS software is used. From these results, the equivalent SIF [6] is evaluated. If the maximum equivalent SIF

$$K_{\mathrm{eq}} = \frac{K_{\mathrm{I}}}{2} + \frac{1}{2}\sqrt{K_{\mathrm{I}}^2 + 4 \cdot (1.155 \cdot K_{\mathrm{II}}^2) + 4 \cdot K_{\mathrm{III}}^2} \leq K_{\mathrm{Id}} \tag{1}$$

reaches the fracture toughness, an unstable crack growth in the wheel occurs.

Many simulations have been done in order to consider different operating conditions, different rail-wheel position, different crack tip position, different interference fit and variable cross-section geometry profile of the RW. From each simulation, SIFs are gathered and equivalent SIFs are evaluated. These results are compiled to graphs in Matlab software (Mathworks Inc, Massachusetts, USA). Three main spots on RW disc are studied, see also Fig. 1.

The first set of acquired graphs shows dependability of the equivalent SIF K_{eq} on rail-wheel position and location of SIFs on the crack tip. Examples of these results can be seen in Fig. 5. These examples represent situation where the crack tip position is 330 mm in RW discs for all considered shapes and for the case of interference fit H7/r6. In these graphs the case of rectilinear train ride is shown. It is important to notice that all graphs have typical regular "V-shape". It is because the crack with the straight radial direction is considered. For the case of rectilinear ride, graphs are symmetric according to the crack mouth. For the case of braking, the graph is non-symmetric, as can be noticed in Fig. 6. The slope shape in all graphs is main function of disc shape, rail position because of the crack mouth, case of ride and the crack position.

For the case of rectilinear ride and for the skew disc cross-section profile, minimum values of equivalent SIF near to $25\ \mathrm{MPa} \cdot \mathrm{m}^{1/2}$ are obtained. Contrary to this, the maximum values near to $40\ \mathrm{MPa} \cdot \mathrm{m}^{1/2}$ are obtained for case of the arc cross-section disc profile, Fig. 5. For the case of braking in Fig. 6, it can be observed that this case of ride does not have any significant influence despite the fact that shapes of graphs are different, but not symmetric because of the zero RW position.

In order to get better summary of all results, graphs of maximum reached values of equivalent SIFs for all types of train ride and all types of cross-section of the RW discs are plotted. These graphs show tendency of the crack behaviour for variable crack length and for different cross-sections (Fig. 7).

Two similar graphs can be seen in Fig. 7. The Fig. 7a) is for the case of accelerating and braking and the Fig. 7b) shows the case of rectilinear ride. The straight primary crack in radial direction is simulated. It is clear from the results that the accelerating and the braking case of the ride are the same. As can be seen in Fig. 7, the tangential forces are less essential.

Hereafter, the other case of interference fit H7/u6 has been studied. As can be noticed in graphs in Fig. 8, higher value of interference fit has major influence on the crack behaviour in the RW disc. The fit H7/u6 highly raises SIFs values in comparison with previously studied interference fit H7/r6. For illustration see graphs for the case of accelerating presented in Fig. 8.

4. Conclusions

In this study, the crack analysis with consideration of mechanical compliance analysis for different types of the cross-section RW disc and operating conditions is preformed. The major

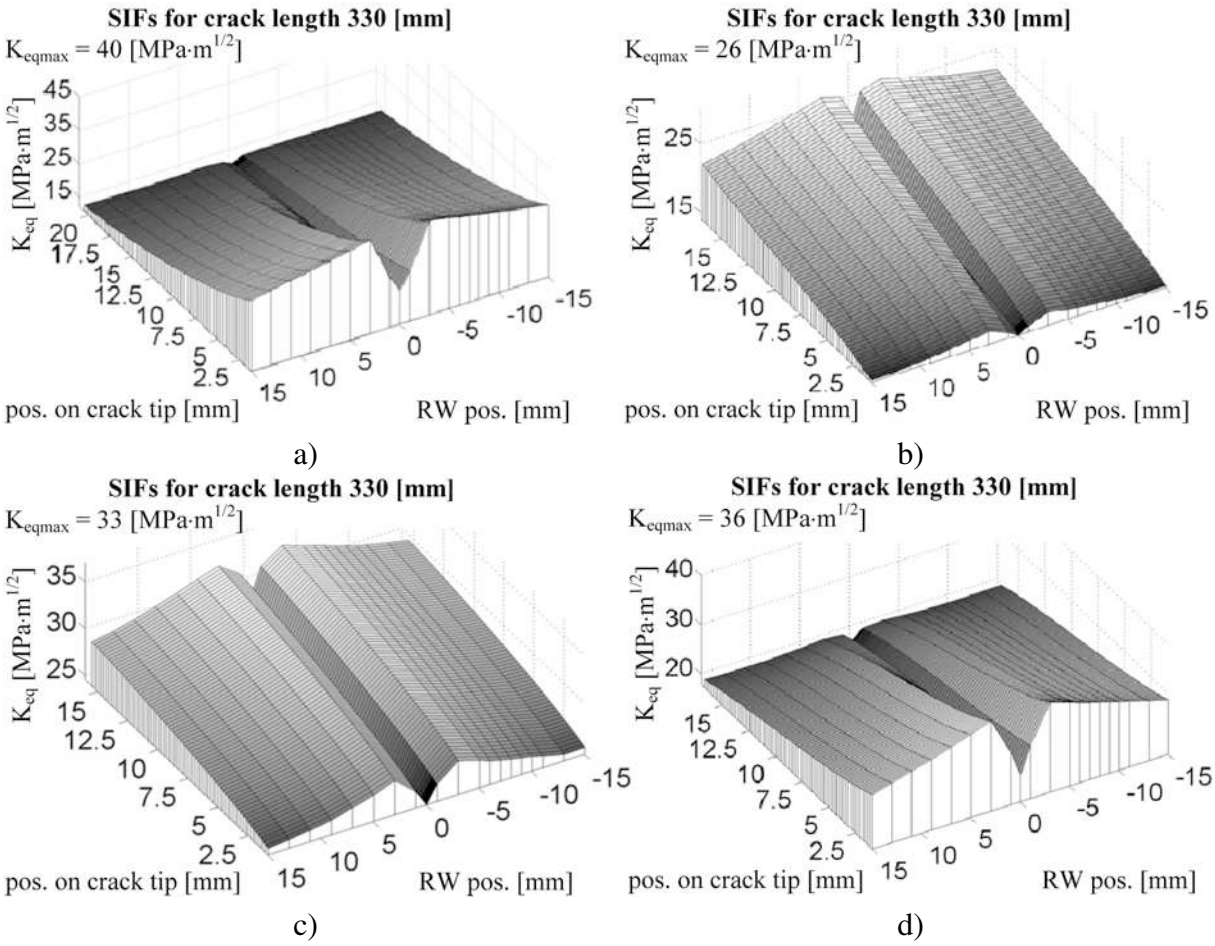

Fig. 5. Set of graphs for rectilinear ride of train for interference fit H7/r6 for disc profiles: a) arc profile, b) skew profile, c) straight profile, d) classic profile

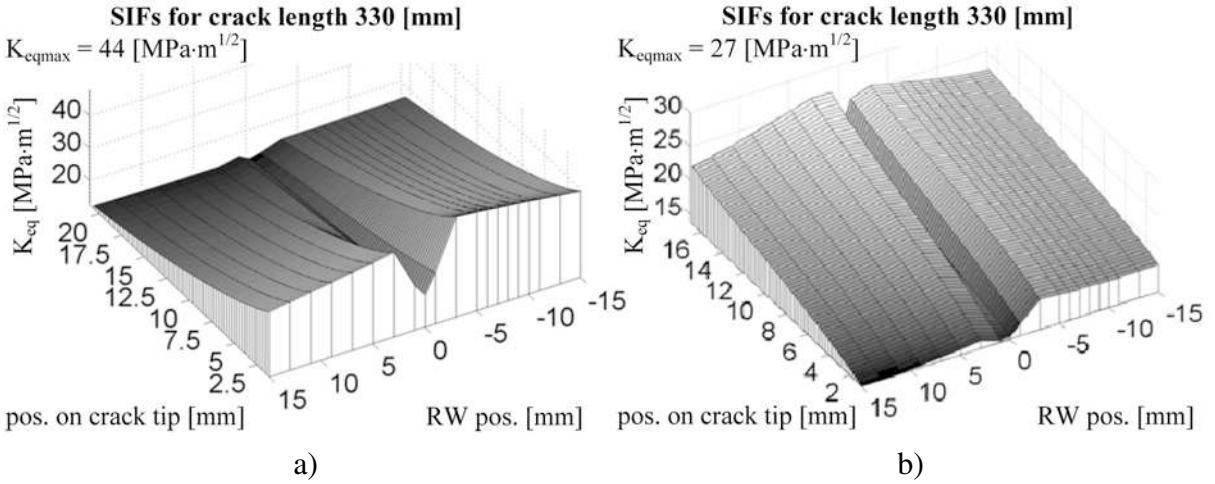

Fig. 6. Selection of graphs for case of braking for interference fit H7/r6 for disc profiles: a) arc profile, b) skew profile

influence on the crack behaviour has value of interference fit and RW loading. The cases of accelerating and braking are less essential. The difference of SIFs between considered interference fits is near to $25\ \mathrm{MPa} \cdot \mathrm{m}^{1/2}$.

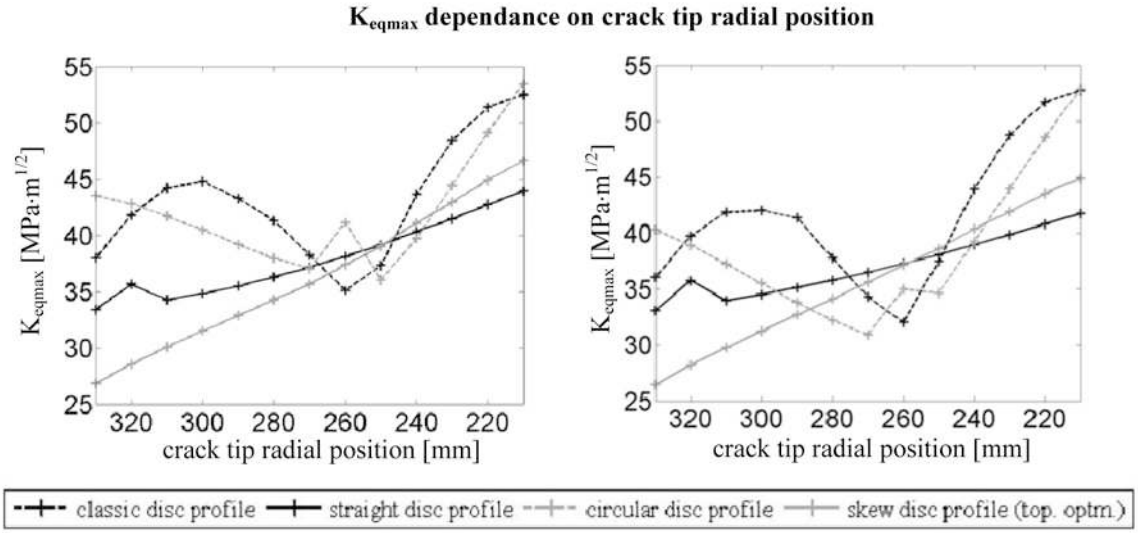

a) b)

Fig. 7. 2D graphs of maximum values K_{eq} from sets of 3D graphs for fit H7/r6: a) braking/accelerating, b) rectilinear ride

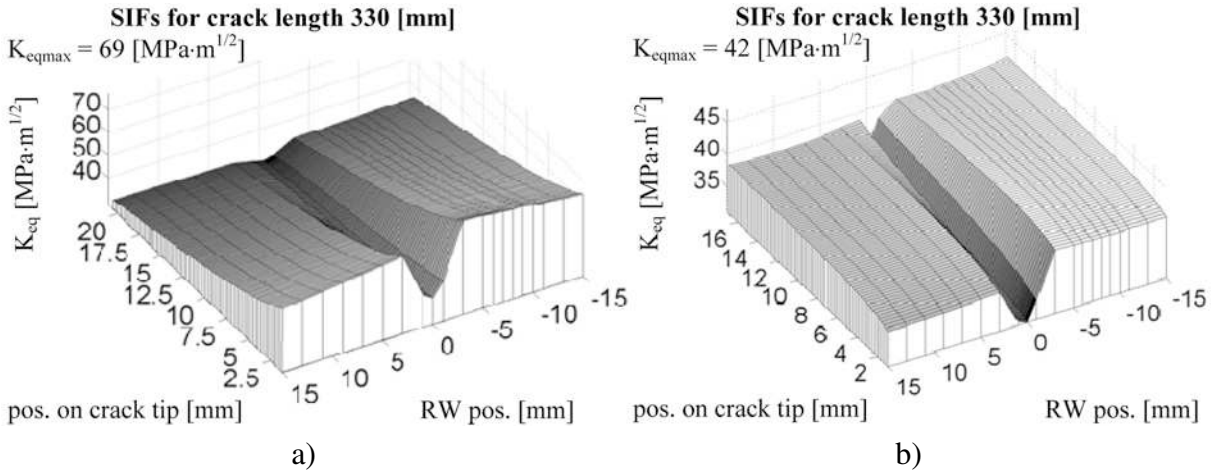

a) b)

Fig. 8. Set of graphs for accelerating ride of train for interference fit H7/u6: a) arc profile, b) skew profile

For better summary of suitability of wheel profiles, it is necessary to consider influence of SIFs and mechanical compliance. As the results show the skew-shaped profiles have the best stiffness and the best crack behaviour near the RW rim. On the contrary, the currently used profile has better mechanical compliance and the crack behaviour is nearly the best in the middle part of the RW disc.

Acknowledgements

The authors are grateful for the support provided by the research project FSI-S-11-11/1190.

References

[1] Ekberg, A., Sotkovszki, P., Anisotropy and rolling contact fatigue of railway wheels, International Journal of Fatigue 23(1) (2001) 29–43.

[2] Jandora, R., Modelling of railway vehicle movement considering non-ideal geometry of wheels and rails, Applied and Computational Mechanics 2(1) (2007) 489–498.

[3] Janíček, P., System approach of selected fields for technicians — Searching for context, CERM, Brno, 2010. (in Czech)

[4] Plank, R., Kuhnb, G., Fatigue crack propagation under non-proportional mixed mode loading, Engineering Fracture Mechanics 62(2–3) (1999) 203–229.

[5] Pook, L. P., Crack Paths, WIT Press, London, 2002.

[6] Richard, H. A. and coll., Development of fatigue crack growth in real structures, Engineering Fracture Mechanics 75(3–4) (2008) 331–340.

[7] Wallentin, M., Bjarneheda, H. L., Lundén, R., Cracks around railway wheel flats exposed to rolling contact loads and residual stresses, Wear 258(7–8) (2005) 1 319–1 329.